buildings

MDPI

Article

Experimental Study and Damping Effect Analysis of a New Tuned Liquid Damper Based on Karman Vortex Street Theory

Hongmei Ren [1], Qiaoqiao Fan [2] and Zheng Lu [2,3,*]

[1] School of Digital Construction, Shanghai Urban Construction Vocational College, Shanghai 200438, China
[2] Department of Disaster Mitigation for Structures, Tongji University, Shanghai 200092, China
[3] State Key Laboratory of Disaster Reduction in Civil Engineering, Tongji University, Shanghai 200092, China
* Correspondence: luzheng111@tongji.edu.cn

Abstract: In order to solve the shortcomings of traditional TLDs (tuned liquid dampers), such as their narrow frequency bands and their occupation of large amounts of space, based on deep-water theory, a new type of TLD incorporating Karmen vortex street theory is proposed and named as KV-TLD. A shaking table experimental test is conducted to fully analyze its vibration damping characteristics and its effectiveness in terms of vibration control is confirmed. Through comparison with a traditional TLD, the superiority of KV-TLD is verified. By analyzing parameters such as the mass ratio and the frequency ratio, it is found that a larger mass ratio means a better damping effect. When the frequency ratio is close to 1.0, the damping effect is better, while the vibration damping advantage of KV-TLD is much lower. Good performance in terms of installation, a wide frequency band, and damping effect means that KV-TLD is superior in terms of actual engineering application possibilities, and can also act as a good reference for subsequent engineering projects.

Keywords: Karman vortex street; tuned liquid dampers; acceleration response; damping effect

Citation: Ren, H.; Fan, Q.; Lu, Z. Experimental Study and Damping Effect Analysis of a New Tuned Liquid Damper Based on Karman Vortex Street Theory. *Buildings* **2023**, *13*, 1013. https://doi.org/10.3390/buildings13041013

Academic Editor: Ramadhansyah Putra Jaya

Received: 5 March 2023
Revised: 3 April 2023
Accepted: 4 April 2023
Published: 12 April 2023

1. Introduction

With the development of high-rise buildings and high-strength materials, structures have become increasingly more sensitive to strong excitation forces, such as winds and earthquakes. Therefore, structural vibration control has received increasing attention in recent years. Among them, a tuned liquid damper (TLD) is a common structural vibration control device due to its advantages in terms of economy, simplicity, and versatility [1–3].

TLDs were firstly used in aerospace engineering and marine technology, such as the rocket fuel tanks (filled with liquid fuel) on rockets and the rocking-reduction water tanks of ships. Subsequently, TLDs have been used in offshore platforms. In 1979, Vandiver et al. [4] firstly used liquid storage tanks on fixed offshore platforms as TLDs and verified the vibration control effect of TLDs. Bauer [5] proposed a new type of damper to suppress the vibration response of structures, which relied on the motion of the intersection of the two layers of liquids. In 1986, researchers introduced TLDs into ground structures and, in 1987, TLD was first applied to the wind vibration control of a ground structure, the command tower of Nagasaki Airport in Japan [6]. Since then, the study of TLDs for control of the dynamic responses of ground structures has attracted greater attention from scholars and engineering designers in civil engineering.

M.J. Tait et al. [7] focused on unidirectional and bidirectional tuned liquid dampers (TLDs) under random excitation and confirmed the effectiveness of these two TLDs. Shadman et al. [8] placed emphasis on the shape of TLDs and analyzed V-shaped and U-shaped TLDs. Considering the wind force, especially for tall buildings, K.W. Min [8] proposed a design procedure to determine the geometrical configurations of the damper size. Lou et al. [9] analyzed the damping rate and the vibration control capacity of TLDs under a rigid basement through the shaking table testing of steel frames, verifying the effectiveness and

superiority of TLDs. J.K. Yu et al. [10] numerically modelled TLDs and compared results with experimental data [11]. In order to compare the seismic performance between TLDs and tuned liquid column dampers (TLCDs, which can be regarded as a new type of TLD), some scholars have conducted both experimental and numerical investigations [12,13]. Yokohama Marine Tower [14] (Japan), Nagasaki Airport Tower [15] (Japan), the Jinshan building (China), the International Trade Building of Dalian (China) [16,17], and many other tall buildings have all been installed with TLDs for vibration control. Various new types of TLDs have been proposed and studied [18–21].

According to the ratio of the depth of the water in the tank and the length of the tank, along with the vibration direction, vibration control theory of TLDs can be subdivided into shallow-water theory and deep-water theory [16,17,22]. When the ratio of the depth of the water in the tank and the length in the tank vibration direction is less than 1/8, the tank is regarded as a shallow-water tank, and vice versa is regarded as a deep-water tank. Due to the shallow depth of water in shallow-water theory, considering the nonlinearity of the liquid motion, the liquid surface oscillation is large enough to increase the damping of the structure, generating a larger dynamic water pressure. Hence, it is relatively more ideal for the damping effect than deep-water tanks with the same mass. Most of the actual projects installed with TLDs choose shallow-water tanks to reduce the wind vibration response. However, even minor changes to a shallow-water tank will have a negative effect on vibration control, meaning that shallow-water tanks need to be specially constructed and the water depth should be strictly controlled. Therefore, the number of shallow water tanks is greater (especially in high-rise buildings), and they occupy a larger space, which directly increases the cost of the project.

The main assumption of deep-water theory is that the liquid surface motion is micro-amplified with linear theory to portray the movement of the liquid. Correspondingly, a deep-water tank can be easily modified with a living water tank, meaning that not only is there no need to install a special tank, but also that there is no need for additional holding space. Hence, TLDs in deep-water theory have the advantages of low cost, easy installation, and are especially suitable for high-rise buildings. However, a deep-water tank has a generally lower level of damping of liquid sway and a narrow frequency band, which makes the control effect much more sensitive to the level of frequency de-tuning, resulting in it being difficult to directly apply this type of TLD in engineering.

Therefore, in this paper, in order to pay full attention to the advantages of deep-water TLDs and to solve their problems (such as narrow frequency bands, etc.), a new deep-water TLD based on Karman vortex street theory, named KV-TLD, is proposed. The vibration damping effect is verified through shaking table tests. Meanwhile, the vibration control performance of KV-TLD is investigated by conducting experiments on several working conditions to explore its engineering application prospects.

2. Design of KV-TLD

2.1. Basic Information about Karman Vortex Street

In a certain range of Reynolds numbers (Re), the bypassing motion of fluid will produce the phenomenon of vortex separation. When the fluid flows around the non-streamline column, vortex separation will be more intense. Due to the instability of the boundary layer, the flow separation generated by the vortex has a certain pattern. When Re is greater than a certain value, there is a special condition: on one side of the column, the vortex can form and separate, while on the other side, is not possible to form vortices and this side can only enter into a stage to prepare for the formation and separation of the vortex; only after the vortex on one side leaves the column at a certain distance can the vortex on the other side form and separate. Hence, the formation of an alternating regular vortex column on both sides of the column, known as the Karmen vortex street and referred to as the vortex street (vortex street), is formed [23–25]. Figure 1 shows the schematic of the vortex street.

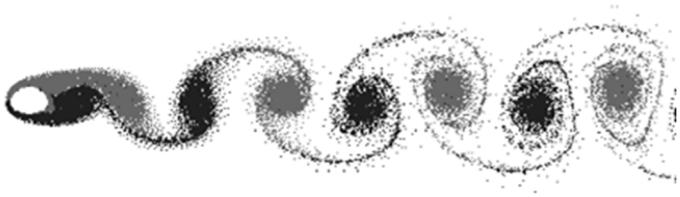

Figure 1. Schematic of the vortex street.

Through the arrangement of the cylindrical bluff body in the deep-water tank to form the Karmen vortex street, the flow resistance can be increased, thus greatly increasing the energy consumption; meanwhile, when the fluid passes through the cylindrical bluff body, the difference in dynamic water pressure on both sides will increase, and the deep-water damping effect can be greatly improved.

2.2. Design of KV-TLD

The KV-TLD consists of five parts: the container, the cylindrical bluff body, the streamline body, the fluid, and the partition, which are shown in Figures 2 and 3.

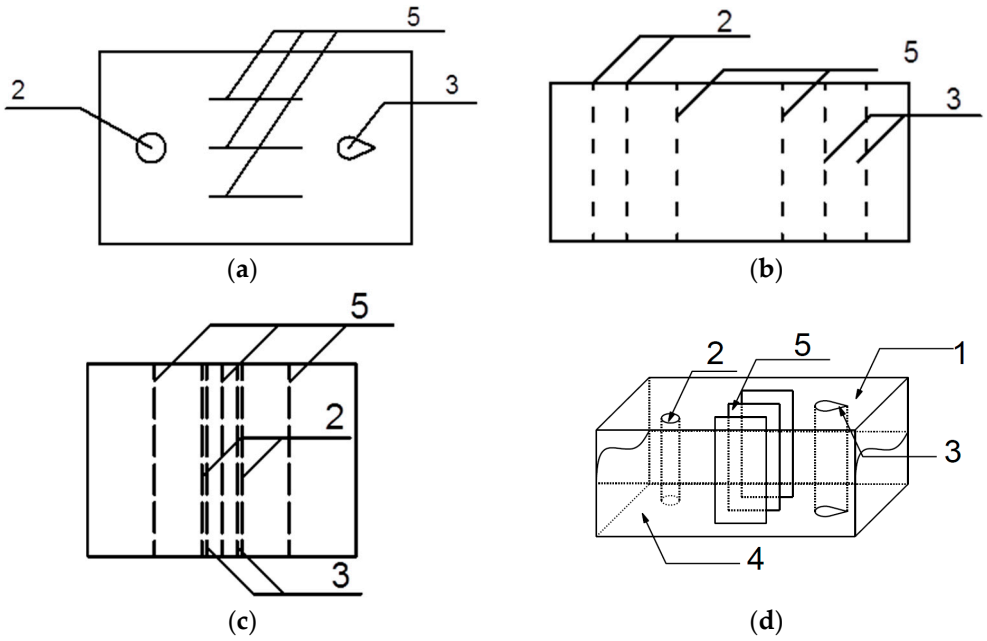

Figure 2. Design of KV-TLD: (**a**) plane; (**b**) front elevation; (**c**) left side elevation; (**d**) 3D. Note: 1–container; 2—cylindrical bluff body; 3—streamline body; 4—fluid (in the experiment of this paper, fluid means water); 5—rectangular partition.

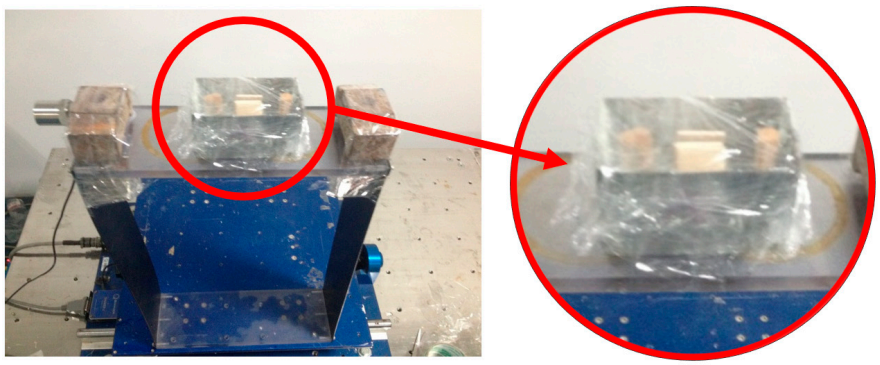

Figure 3. Picture of KV-TLD and the whole experimental device.

The container is a deep-water tank, the ratio of the fluid depth to the length in the container's vibration direction is larger than 1/8. The fluid in the container is water. The water provides the structural restoring force to the side pressure of the vessel and reduces the structural amplitude. The cylindrical bluff body is fixed on the left side of the container (Figure 2a) and the specific sizes are determined according to the actual situation of the load on the damped structure, so as to control the Re to form the Karmen vortex, to increase energy consumption, and to finally improve the damping effect. The rectangular partitions are fixed in the middle of the container to increase the flow path of the water and increase the shaking damping. The streamline body is fixed on the right side of the container to speed up the flow of the water and increase the duration of the reciprocating motion, thus increasing energy consumption.

3. Experiment and Performance Analysis

In order to verify the damping effect of KV-TLD, this paper adopts the single degree-of-freedom (SDOF) structure (steel frame) for experimental testing, and provides a more in-depth understanding of the performance of this newly proposed TLD.

Based on comparative experiments, the acceleration response under various controlled conditions are compared with traditional TLDs. Furthermore, the influencing factors affecting the damping efficiency (such as mass ratio and frequency) are analyzed and summarized.

3.1. Experiment

In the experimental test, the container of the KV-TLD has five sizes of steel boxes, all of which are uniformly 60 mm in height, 60 mm in width, and 80 mm, 100 mm, 120 mm, 140 mm, and 160 mm in length, respectively.

The experiment uses a single-story shear-type frame structure model (32 cm in length, 11 cm in width, 50 cm in height) with two columns made of steel plates (2 mm in thickness) on both sides and a floor slab made of Plexiglas (3 mm in thickness). The dynamic characteristics are shown in Table 1.

Table 1. Structural dynamic characteristics.

Total Height of the Whole Structure/cm	Weight/kg	Frequency/Hz	Lateral Stiffness/(N/m)
53	1.60	2.5	500

Figure 3 shows the test device and setup of the experiment. The ground vibrations and swept loads in the test were generated using a Shaker II mini-shaker. It is a standard small shaker test equipment adopted in civil engineering tests as its quality and vibration simulation capacity can both reach the research requirements. The maximum loading value of a Shaker II mini-shaker is 15 kg, and the maximum acceleration it can provide is 2.5 g. The acceleration response is collected by an acceleration sensor (named as: Ua3000 acquisition equipment) and the sample frequency is 50 Hz. The system consists of sensors, multi-channel collectors, and acquisition and analysis software (based on the VB.Net platform).

There are five different sizes of containers, and the detailed parameters of which are shown in Table 2. The frequency ratio in Table 2 is the ratio of the frequency of the KV-TLD to the fundamental frequency of the structure. The mass ratio (the ratio of the damper's mass to the structure's mass) is one of the main factors influencing the action of the TLD-structure system. The formula for calculating the damping rate is shown in Equation (1).

Table 2. Parameters of the KV-TLD.

Length of Container/cm	Mass Ratio/%	Water Depth/cm	Frequency/Hz	Frequency Ratio
8	2	2.33	2.66	1.93
8	3	3.50	2.93	2.12
8	4	4.67	3.04	2.21
10	2	1.87	2.03	1.47
10	3	2.80	2.35	1.70
10	4	3.73	2.54	1.84
12	2	1.56	1.58	1.15
12	3	2.33	1.88	1.36
12	4	3.11	2.09	1.51
14	2	1.33	1.27	0.92
14	3	2.00	1.53	1.11
14	4	2.67	1.73	1.25
16	2	1.17	1.05	0.76
16	3	1.75	1.27	0.92
16	4	2.33	1.45	1.05

The width (6 cm) and minimum/maximum lengths (8 cm/16 cm) of the container are determined by the width and length of the structure itself, as they cannot exceed the structure's geometry. In the range of 8 cm~16 cm, five classes of length at spacings of 2 cm are set up. In order to ensure that the depth of the TLD can meet the requirement of "deep-water", the depth of the liquid needs to be larger than 1/8 of the container's length of vibration direction. Hence, the critical mass ratio can be calculated, and the results are between 0.86%~1.71%; thus, the three mass ratios adopted in this paper are: 2%, 3%, and 4%.

$$damping\ rate = \frac{responses(without\ control) - reponses(under\ control)}{responses(without\ control)} \quad (1)$$

Sine wave, Kobe wave, and El-Centro wave were used as inputs at the bottom of the structure, respectively; 1.38 Hz was selected for the sine wave frequency input to investigate the vibration damping effect under resonance. The amplitude of each waveform was 3 cm. In addition, the peak (AMP) acceleration and root mean square (RMS) acceleration at the top of the main structure were mainly adopted as the key parameters to estimate the performance of the traditional TLD and the KV-TLD in the subsequent analysis.

3.2. Effectiveness Demonstration and Influence of Mass Ratio

The experimental data are shown in Table 3. It can be confirmed that all damping rates in Table 3 are larger than 0, meaning that the newly proposed damper, KV-TLD, can indeed have a positive effect on vibration control.

Figure 4 shows the acceleration curves with different mass ratios and wave types. Although the amplitude of the damping rate varies for different waves (input), KV-TLDs can still have significant damping effects in all conditions. The damping rate under the El-Centro wave is generally more obvious than those of the other two waves, and the largest damping rate (nearly half) is achieved under the conditions of the El-Centro wave and a 4% mass ratio.

Table 3. Experimental data (mass ratio).

Wave Type	Mass Ratio/%	Acceleration (Without Control)/(cm/s^2)		Acceleration (KV-TLD)/(cm/s^2)		Damping Rate/%	
		Peak (AMP)	Root Mean Square (RMS)	Peak (AMP)	Root Mean Square (RMS)	Peak (AMP)	Root Mean Square (RMS)
sine	2	26.1841	18.0580	22.0993	13.7954	23.61	15.60
	3	26.1841	18.0580	19.0563	12.4453	31.08	27.22
	4	26.1841	18.0580	18.5545	12.0399	33.33	29.14
El-Centro	2	10.8815	3.855	9.4034	2.8205	26.84	13.58
	3	10.8815	3.855	8.6370	2.4578	36.24	20.63
	4	10.8815	3.855	8.7494	2.3931	37.92	19.59
Kobe	2	12.2715	2.5610	11.0463	2.0815	18.72	9.98
	3	12.2715	2.5610	10.4682	1.8743	14.7	27.39
	4	12.2715	2.5610	10.1426	1.9176	17.35	30.26

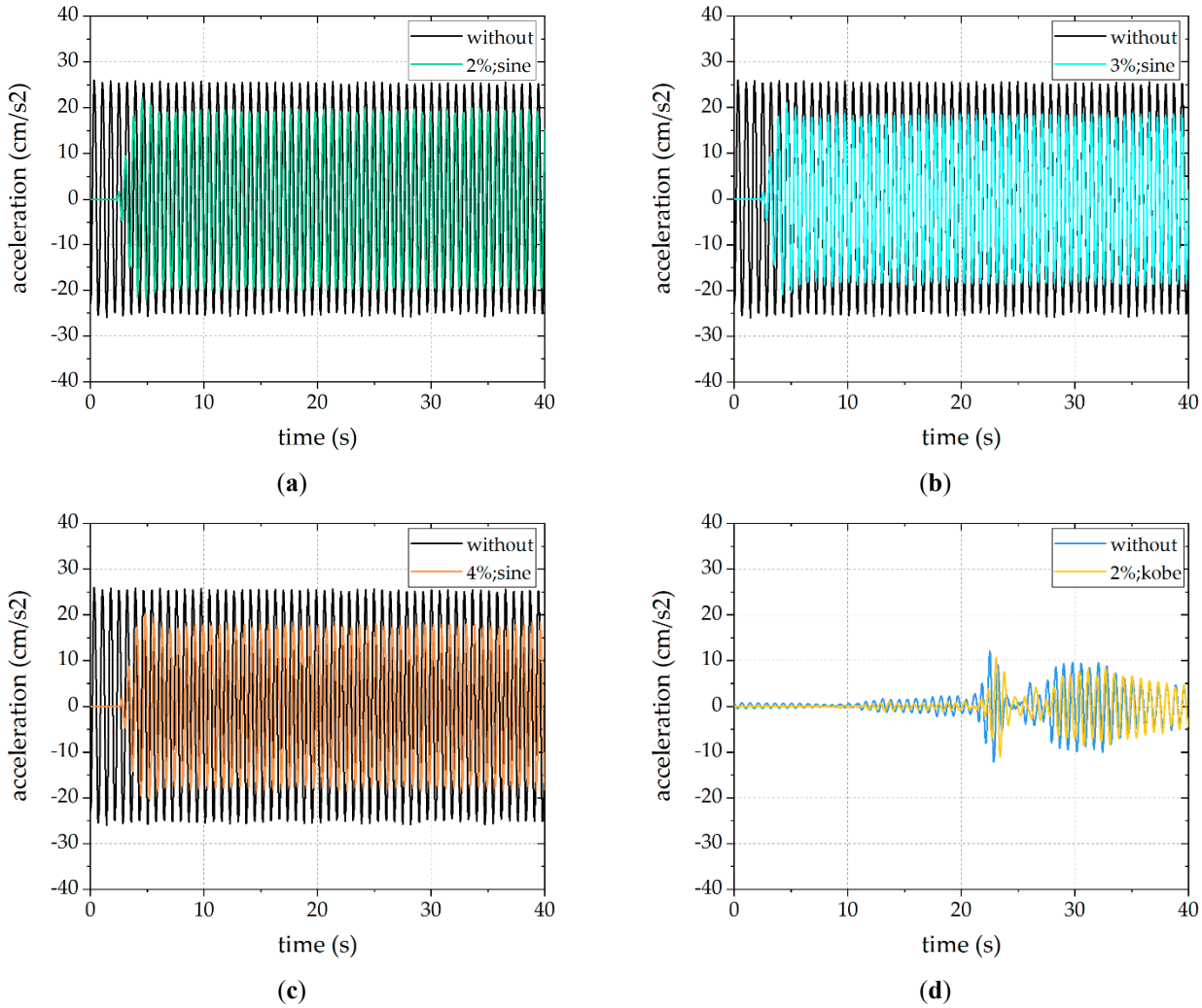

Figure 4. *Cont.*

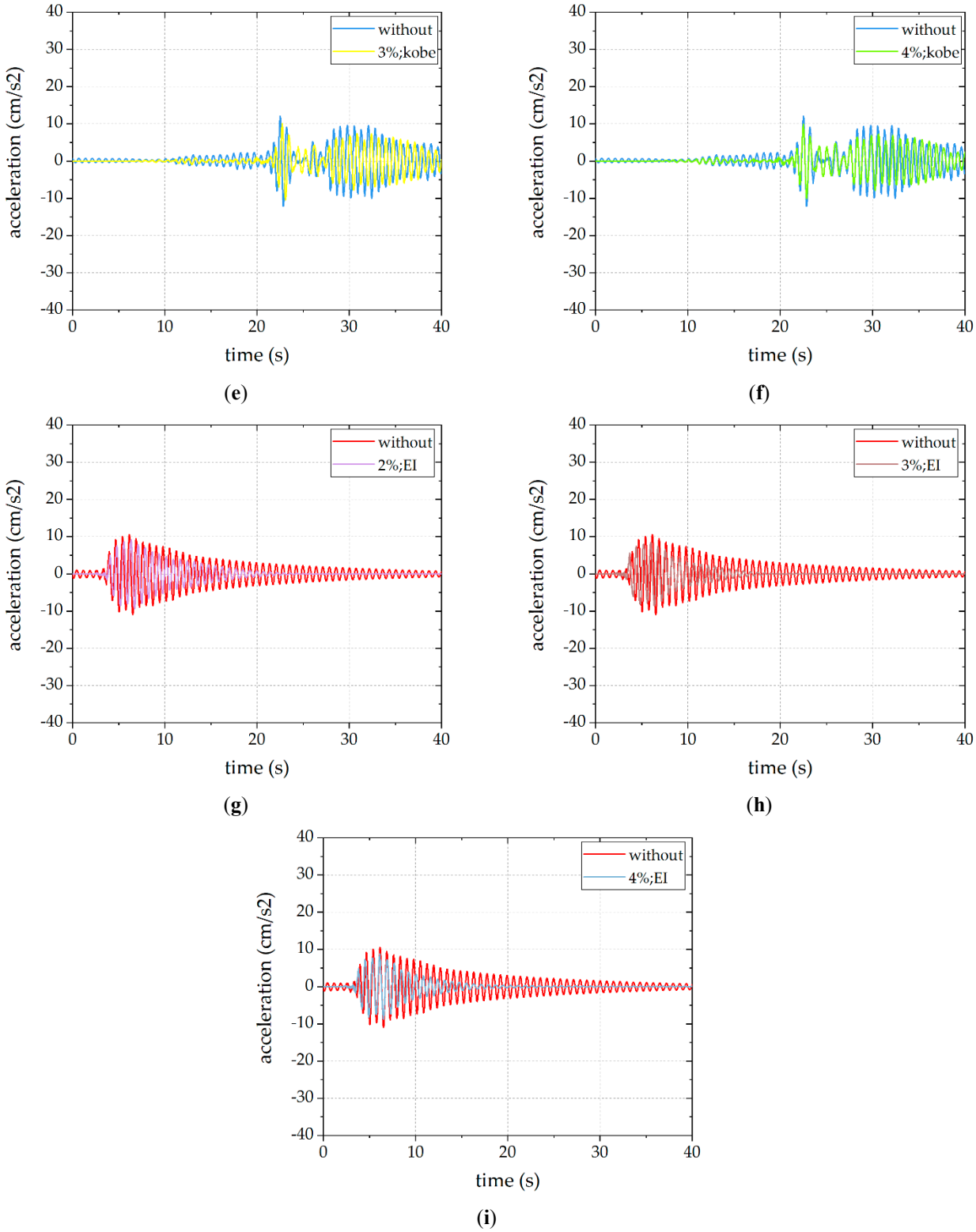

Figure 4. Acceleration time curve (2%, 3%, and 4% are mass ratios): (**a**) sine; 2%; (**b**) sine; 3%; (**c**) sine; 4%; (**d**) Kobe; 2%; (**e**) Kobe; 3%; (**f**) Kobe; 4%; (**g**) El-Centro; 2%; (**h**) El-Centro; 3%; (**i**) El-Centro; 4%. Note: to simplify the image annotation, "El" in figures is used to represent the El-Centro wave, "sine" means sine wave, "kobe" means Kobe wave; and the remaining figures are the same.

Figure 5 shows the comparison results of different mass ratios under various wave types. When the input wave is sine, the AMP and RMS damping rates both gradually

increase along with the mass ratio, and the damping effects become increasingly greater. The AMP damping rate of the El-Centro wave increases with the mass ratio, reaching 37.92% at a mass ratio of 4%; the RMS damping rate of the El-Centro wave increases from 2% to 3%, but slightly decreases from 3% to 4%. Under the action of the Kobe wave, the RMS damping rate monotonically increases, while the AMP damping rate firstly decreases and then increases along with the increase in the mass ratio.

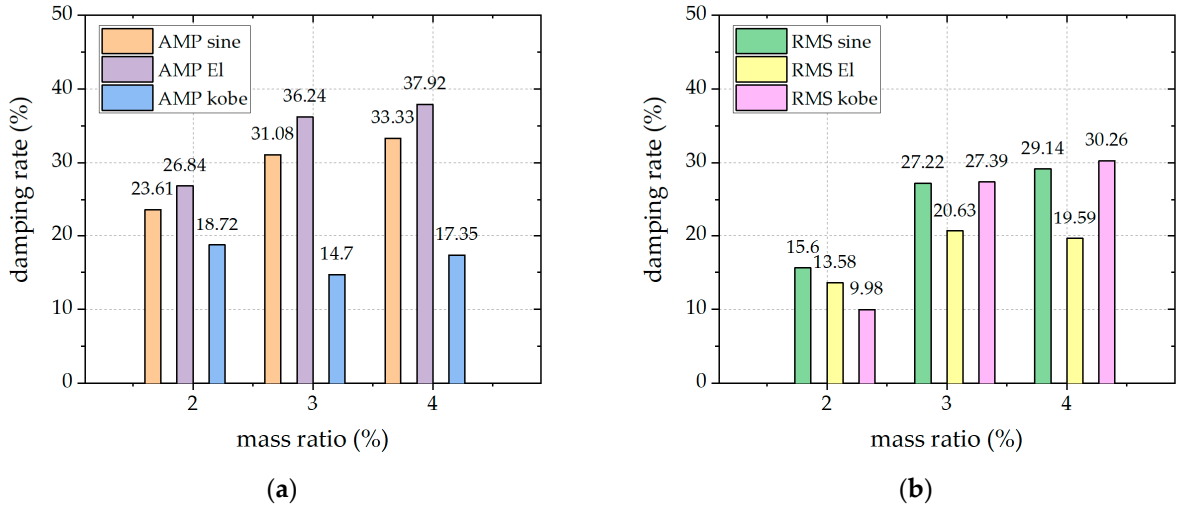

Figure 5. Influencing factor: mass ratio: (**a**) AMP (peak); (**b**) RMS (root mean square).

In general, under the condition that other parameters remain unchanged, the larger the mass ratio, the better the damping effect of KV-TLD, which is in accordance with the traditional TLD theory. However, it should be noted that this effective damping effect slowly decreases as the mass ratio increases; i.e., the increase in damping effect is not linearly related to the increase in the mass ratio. In practical engineering, it is necessary to not only consider the damping effect of the damper, but also the "burden" of the damper mass itself on the structure; too large a mass ratio may also have some negative effects on the structural displacement.

In engineering application, the appropriate mass ratio can be selected according to multiple considerations and combined with the water consumption demand of the building to achieve the ideal damping effect.

3.3. Superiority of KV-TLD and Influence of Frequency

From the theoretical analysis, it is known that the best damping effect of the TLD is achieved when the frequency of the traditional TLD is tuned to be close to the structure's fundamental frequency. Due to the internal optimization design of vortex street theory adopted in KV-TLD, the liquid flow state and energy dissipation mechanism differ from traditional TLDs, and the damping law may deviate from the traditional theory.

In this section, the effect of the KV-TLD is calculated under different frequency ratios, and a comparison with the traditional TLD is conducted to investigate the newly proposed TLD's vibration damping characteristics. The detailed frequency information is listed in Table 2.

3.3.1. Superiority of KV-TLD

The comparation results are shown in Table 4. Table 4 shows the vibration damping advantage results (the vibration damping advantage equals the damping rate of the KV-TLD minus the damping rate of the TLD). It can be seen that, although under individual conditions, the vibration damping advantage values are negative; vibration damping advantage values in Table 4 are basically positive (larger than 0), indicating that the damping effect of KV-TLD is better than that of the traditional TLD.

Table 4. Vibration damping advantage.

Mass Ratio/%	2%			3%			4%		
Wave Type	**Frequency Ratio**	**AMP/%**	**RMS/%**	**Frequency Ratio**	**AMP/%**	**RMS/%**	**Frequency Ratio**	**AMP/%**	**RMS/%**
sine	1.93	6.39	7.42	2.12	9.98	8.87	2.21	7.64	7.55
	1.47	7.05	7.29	1.70	7.08	6.13	1.84	9.45	10.14
	1.15	7.60	6.84	1.36	7.64	6.15	1.51	2.78	7.03
	0.92	−0.01	0.04	1.11	0.91	0.99	1.25	3.47	−0.75
	0.76	3.85	2.42	0.92	2.34	2.01	1.05	2.12	2.05
El-Centro	1.93	1.11	0.56	2.12	6.02	7.71	2.21	3.50	2.35
	1.47	3.08	5.34	1.7	3.61	4.13	1.84	8.37	8.33
	1.15	1.76	2.78	1.36	3.98	3.53	1.51	6.04	3.60
	0.92	0.53	−2.61	1.11	1.27	−0.66	1.25	−5.28	−2.90
	0.76	0.66	2.58	0.92	1.92	−2.81	1.05	−2.54	−5.46
Kobe	1.93	1.66	3.26	2.12	1.20	9.85	2.21	6.45	1.94
	1.47	9.29	4.26	1.7	3.59	4.01	1.84	1.83	2.30
	1.15	4.92	2.35	1.36	2.15	2.62	1.51	3.00	1.69
	0.92	3.78	−3.00	1.11	2.01	−0.04	1.25	−3.44	5.71
	0.76	6.55	2.32	0.92	2.59	−0.58	1.05	0.12	−5.13

3.3.2. Influence of Frequency Ratio

There are three mass ratios adopted in this paper: 2%, 3%, and 4%.

When the mass ratio is 2% (Figure 6), the AMP damping rates of all waves monotonically increase when the frequency ratio is between 0.76 and 0.92. At a frequency ratio between 0.92 to 1.93, the AMP damping rate of each wave monotonically decreases. The AMP damping rate can reach the maximum value at a frequency ratio of 0.92.

The results of the RMS damping rates of the sine wave and the Kobe wave basically conform to the above rule. The El-Centro wave is slightly different, and the RMS damping rate increases at between frequency ratios of 1.47 to 1.93, which is still at a lower level than the value when the frequency ratio is 0.92. In general, the damper system has the best damping effect when the frequency of the damper and the frequency of the structure are equal. However, considering that the damper itself also has a certain mass and vibration frequency, the installation of the damper will also have an impact on the dynamic characteristics of the structure and many other factors; the frequency ratio that enables the damper to produce the best vibration controlling effect is not exactly equal to 1.0, but should be in the vicinity of 1.0 [26–28]. This explains the phenomena shown in Figure 6a,b.

As for vibration damping advantage (shown in Figure 6c,d), the vibration damping advantage gradually decreases when the frequency is between 0.76 to 0.92. When the frequency ratio is 0.92 (which corresponds to the largest AMP and RMS damping rates), the damping advantages (AMP and RMS) reach the lowest levels, and there are even negative values in some conditions. After that, the damping advantages increase along with the frequency ratio at an average level. The damping advantage is much more significant when the frequency is not near the structure's fundamental frequency.

When the mass ratio is 3% (Figure 7), generally, the closer the frequency ratio is to 1.0, the larger the damping rate. The curve development process is slightly different from the Kobe wave (AMP) and the El-Centro wave (RMS): the damping rate reaches the maximum value at a frequency ratio of 1.36 (Kobe wave) and 1.11 (El-Centro wave), and then decreases.

Figure 7c,d shows the vibration damping advantages when the mass ratio is 3%. Similar to the results at a mass ratio of 2%, there are some conditions that where the advantage values are lower than 0 (although all the damping ratios are larger than 0); on the other hand, the superiority of the KV-TLD to the traditional TLD still exists at an average level. Generally, the vibration damping advantage becomes larger along with the frequency ratio.

As shown in Figure 8, the AMP and RMS damping rates become smaller when the frequency ratio is larger than 1.0, and maintains a lower level overal. In general, when the frequency ratio is much closer to 1.0, the damping effect is much better. Negative values of the damping advantage are observed at frequency ratios of 1.25 and 1.05. The curve of the damping advantage fluctuates more at a mass ratio of 4% compared to at 2% and at 3%.

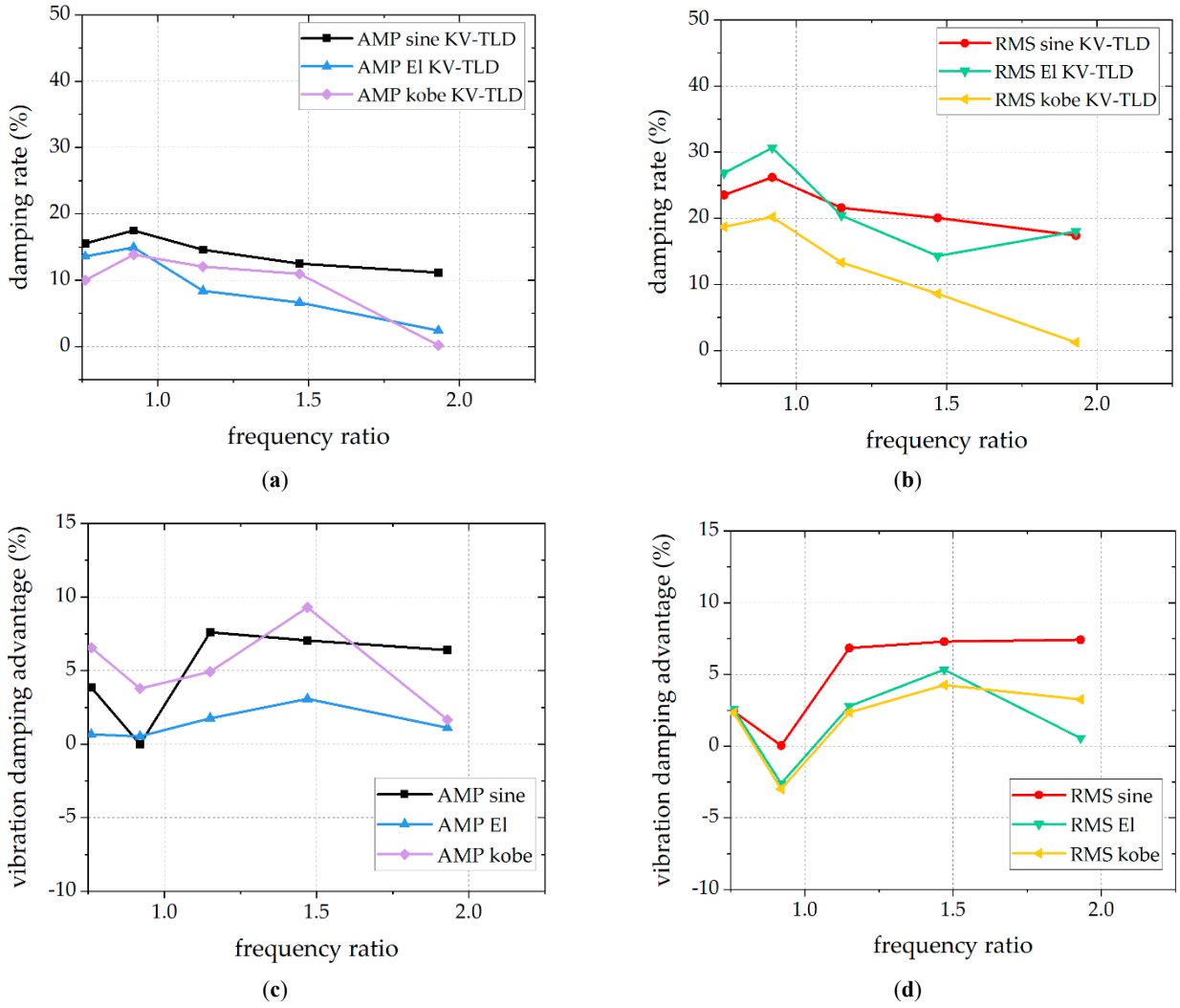

Figure 6. Frequency ratio analysis: mass ratio (2%): (**a**) damping rate (AMP); (**b**) damping rate (RMS); (**c**) vibration damping advantage (AMP); (**d**) vibration damping advantage (RMS).

In summary, there are two main characteristics regarding the influence of the frequency ratio.

Firstly, the closer the frequency ratio is to 1.0, the closer the KV-TLD's frequency is to the structure's fundamental frequency, the higher the damping rate is, and a better damping effect can be reached. This law is consistent with traditional TLDs. In actual engineering projects, the size of the KV-TLD and the depth of fluid shall be determined according to the structure's fundamental frequency in order to give full play to the tuning effect and achieve the best possible damping effect.

Secondly, when placing emphasis mainly on the vibration damping advantage, it can be concluded that when the KV-TLD's frequency is far from the structure's frequency, the damping advantage is more significant; when these two indexes are close to each other, the advantage is smaller, and, even in some conditions, negative values will appear.

Although the vibration damping advantage cannot always be maintained at a high level, compared with traditional TLDs, the KV-TLD can indeed broaden and enlarge the frequency band, as it can cause a better damping effect when the frequency ratio deviates

from 1.0 and the tuning effect is relatively poor. This characteristic has obvious superiority in engineering applications. On the one hand, the damping effect will not significantly change due to the slight change in liquid depth, meaning that there is no need for dedicated maintenance to control and keep the liquid depth unchanged. On the other hand, when the maximum considered earthquake occurs, the whole structure will enter into the elasto-plastic stage and structural elements will yield, crack, and finally become damaged, leading a change in the fundamental frequency of the structure and the frequency ratio moving away from 1.0; at this time, the KV-TLD can still have a significant damping effect that traditional TLDs cannot achieve. In other words, the KV-TLD can address the limitations of traditional TLDs with a wider frequency band as its damping effect can be exerted both into elastic and elasto-plastic stages, and it can be applied in a larger variety of intensities, such as a MCE (maximum considered earthquake), a DBE (designed based earthquake), and a SLE (service level earthquake).

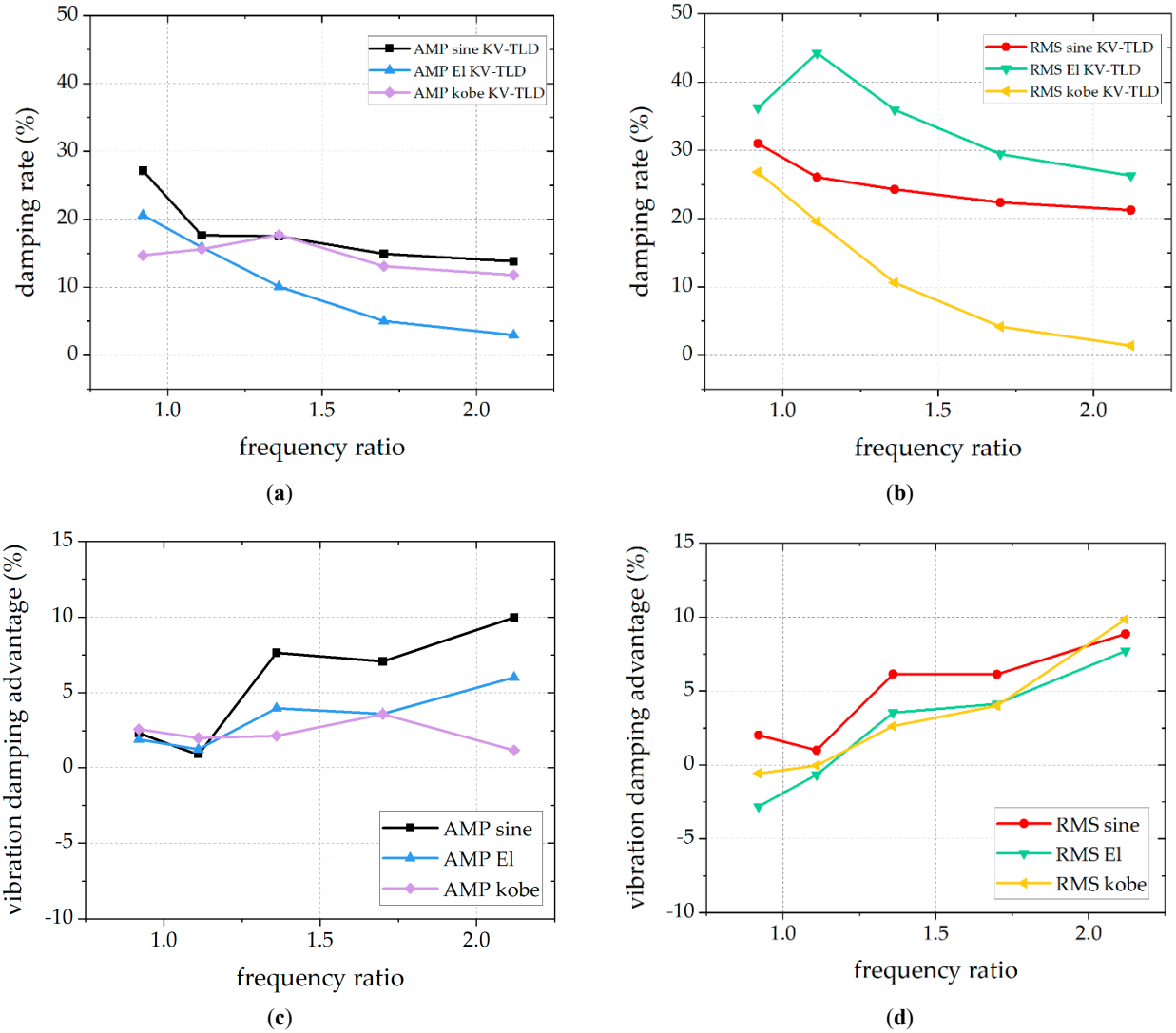

Figure 7. Frequency ratio analysis: mass ratio (3%): (**a**) damping rate (AMP); (**b**) damping rate (RMS); (**c**) vibration damping advantage (AMP); (**d**) vibration damping advantage (RMS).

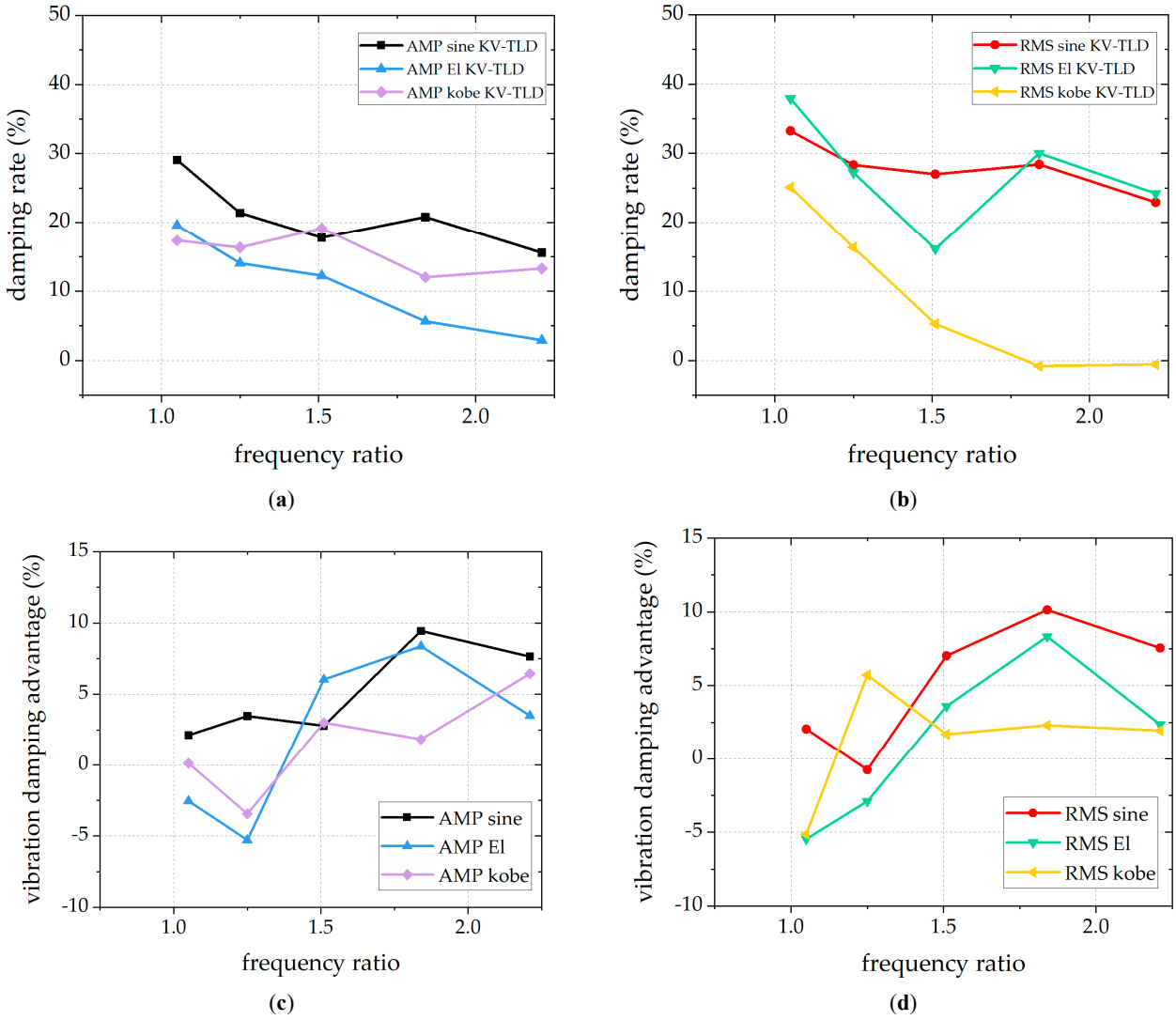

Figure 8. Frequency ratio analysis: mass ratio (4%): (**a**) Damping rate (AMP); (**b**) Damping rate (RMS); (**c**) Vibration damping advantage (AMP); (**d**) Vibration damping advantage (RMS).

4. Conclusions

A new type of TLD (based on Karmen vortex street theory), named KV-TLD, is proposed. Through the adoption of Karmen vortex street theory, the cylindrical bluff body, streamline body, and rectangular partitions are arranged in the container to increase the flow path and form Karmen vortex street theory, which finally improves the damping effect. The vibration damping effect is verified by shaking table tests and is compared with traditional TLDs. The factors (mass ratio and frequency ratio) of KV-TLD influencing the damping effect are investigated by analyzing parameters such as the damping rate and the vibration damping advantage in order to fully explore its engineering application prospects.

The following conclusions can be drawn.

(1) The effectiveness of the KV-TLD is confirmed under the action of sine, El-Centro, and Kobe waves. The AMP and RMS damping rates can both reach an average level of 20%. The damping rate under the El-Centro wave is generally more obvious than those of the other two waves, and the largest damping rate (nearly half) is achieved under the condition of the El-Centro wave and a 4% mass ratio.

(2) In general, under the condition that other parameters remain unchanged, the larger the mass ratio, the better the damping effect of the KV-TLD, which is in accordance with traditional TLD theory. In engineering application, the appropriate mass ratio

can be selected according to this law and can be combined with the water consumption demand of the building to achieve the ideal damping effect.

(3) Under the same conditions, the damping effect of the KV-TLD is basically superior to the traditional TLD (although there are some individual cases where the TLD has better significant damping rate values).

(4) The damping effect is significantly influenced by the frequency ratio. The closer the frequency ratio is to 1.0, the better and more obvious the damping effect is and the lower the damping advantage is. The damping characteristic of the KV-TLD largely solves the problems of a narrow frequency band and sensitivity to the degree of frequency tuning of traditional deep-water TLDs, which greatly increases the feasibility and effectiveness of deep-water TLDs in engineering applications.

There are also limitations which can be further analyzed in the future. For example, a numerical model is an important method as it can not only help to verify the accuracy of experimental data, but can also be used to further supplement the analysis, which the test dose not fully consider. As this paper is a preliminary study, a corresponding numerical simulation study can be carried out in the future. Furthermore, the structure adopted in this paper is SDOF, and, in the future, an investigation of a MDOF (multi-degree of freedom) structure could also be conducted.

Author Contributions: Conceptualization, H.R., and Z.L.; methodology, H.R.; formal analysis, Q.F.; writing—original draft preparation, H.R.; writing—review and editing, Z.L. All authors have read and agreed to the published version of the manuscript.

Funding: Financial support from National Key Research and Development Program of China under Grant No. 2020YFB1901402; National Natural Science Foundation of China (52178296); Program of Shanghai Academic Research Leader (20XD1423900).

Institutional Review Board Statement: Not applicable.

Informed Consent Statement: Not applicable.

Data Availability Statement: Data available on request.

Acknowledgments: Financial support from National Key Research and Development Program of China under Grant No. 2020YFB1901402 is highly appreciated. This work is also supported by National Natural Science Foundation of China (52178296) and Program of Shanghai Academic Research Leader (20XD1423900).

Conflicts of Interest: The authors declare no conflict of interest.

References

1. Symans, M.D.; Constantinou, M.C. Semi-active control systems for seismic protection of structures: A state-of-the-art review. *Eng. Struct.* **1999**, *21*, 469–487. [CrossRef]
2. Haroun, M.A.; Pires, J.A.; Won, A. Active orifice control in hybrid liquid column dampers. In Proceedings of the First World Conference On Structural Control, Los Angeles, CA, USA, 3–5 August 1994.
3. Crewe, A. Passive energy dissipation systems in structural engineering. *Struct. Saf.* **1998**, *20*, 197–198. [CrossRef]
4. Vandiver, J.K.; Mitome, S. The Effect of Liquid Storage Tanks on the Dynamic Response of Offshore Platforms. *J. Pet. Technol.* **1979**, *31*, 1231–1240. [CrossRef]
5. Bauer, H.F. Oscillations of immiscible liquids in a rectangular container: A new damper for excited structures. *J. Sound Vib.* **1984**, *93*, 117–133. [CrossRef]
6. Tamura, Y.; Fujii, K.; Ohtsuki, T.; Wakahara, T.; Kohsaka, R. Effectiveness of tuned liquid dampers under wind excitation. *Eng. Struct.* **1995**, *17*, 609–621. [CrossRef]
7. Tait, M.J.; Isyumov, N.; El Damatty, A.A. Performance of Tuned Liquid Dampers. *J. Eng. Mech.* **2008**, *134*, 417–427. [CrossRef]
8. Shadman, M.; Akbarpour, A.; Asme. Comparative study of utilizing a new type V-Shaped Tuned Liquid Column Damper and U-Shaped Tuned Liquid Column Damper in floating wind turbines. In Proceedings of the 31st ASME International Conference on Ocean, Offshore and Arctic Engineering, Rio de Janeiro, Brazil, 1–6 July 2012; pp. 277–283.
9. Lou, M.; Niu, W.; Zong, G.; Chen, G. Shaking table model test for a steel structure under control of tuned liquid damper. *Earthq. Eng. Eng. Vib.* **2006**, *26*, 145–151.
10. Yu, J.-K.; Wakahara, T.; Reed, D.A. A non-linear numerical model of the tuned liquid damper. *Earthq. Eng. Struct. Dyn.* **1999**, *28*, 671–686. [CrossRef]

11. Reed, D.; Yu, J.; Yeh, H.; Gardarsson, S. Investigation of Tuned Liquid Dampers under Large Amplitude Excitation. *J. Eng. Mech.* **1998**, *124*, 405–413. [CrossRef]
12. Kim, Y.-M.; You, K.-P.; Cho, J.-E.; Hong, D.-P. The vibration performance experiment of Tuned Liquid damper and Tuned Liquid Column damper. *J. Mech. Sci. Technol.* **2006**, *20*, 795–805. [CrossRef]
13. Fei, Z.; Jinting, W.; Feng, J.; Liqiao, L. Control performance comparison between tuned liquid damper and tuned liquid column damper using real-time hybrid simulation. *Earthq. Eng. Eng. Vib.* **2019**, *18*, 695–701. [CrossRef]
14. Fujii, K.; Tamura, Y.; Sato, T.; Wakahara, T. Wind-induced vibration of tower and practical applications of Tuned Sloshing Damper. *J. Wind Eng. Ind. Aerodyn.* **1990**, *33*, 263–272. [CrossRef]
15. Kamgar, R.; Gholami, F.; Zarif Sanayei, H.R.; Heidarzadeh, H. Modified Tuned Liquid Dampers for Seismic Protection of Buildings Considering SoilStructure Interaction Effects. *Iran. J. Sci. Technol. Trans. Civ. Eng.* **2020**, *44*, 339–354. [CrossRef]
16. Hongnan, L.I.; Qinyang, J.; Lichang, W.; Fanlin, L.I. Wind-induced vibration control of dalian international trade center using tuned liquid dampers. *Chin. J. Comput. Mech.* **2007**, *24*, 733–740.
17. Jing, Q.; Li, H.; Wang, L.; Li, F. Wind-induced vibration control of International Trade Building of Dalian using tuned liquid dampers. *Earthq. Eng. Eng. Vib.* **2006**, *26*, 111–118.
18. Zhao, Z.; Zhang, R.; Jiang, Y.; Pan, C. A tuned liquid inerter system for vibration control. *Int. J. Mech. Sci.* **2019**, *164*, 105171. [CrossRef]
19. Pandey, D.K.; Sharma, M.K.; Mishra, S.K. A compliant tuned liquid damper for controlling seismic vibration of short period structures. *Mech. Syst. Signal Process.* **2019**, *132*, 405–428. [CrossRef]
20. Zhang, J.; Kwok, K. Robust design of a new composite tuned liquid damper. In Proceedings of the 14th International Symposium on Structural Engineering (ISSE-14), Beijing, China, 12–15 October 2016; pp. 1050–1055.
21. Hokmabady, H.; Mojtahedi, A.; Mohammadyzadeh, S.; Ettefagh, M.M. Structural control of a fixed offshore structure using a new developed tuned liquid column ball gas damper (TLCBGD). *Ocean Eng.* **2019**, *192*, 106551. [CrossRef]
22. Jin, Q. *Wind-Induced Vibration Control of Dalian International Trade Center Using Tuned Liquid Damper*; Dalian University of Technology: Dalian, China, 2005. (In Chinese)
23. Dong, S.; Triantafyllou, G.S.; Karniadakis, G.E. Elimination of vortex streets in bluff-body flows. *Phys. Rev. Lett.* **2008**, *100*, 204501. [CrossRef]
24. Kim, S.; Alam, M.M.; Maiti, D.K. Wake and suppression of flow-induced vibration of a circular cylinder. *Ocean Eng.* **2018**, *151*, 298–307. [CrossRef]
25. Yao, G.; Wang, H.; Yang, C.; Wen, L. Research and design of underwater flow-induced vibration energy harvester based on Karman vortex street. *Mod. Phys. Lett. B* **2017**, *31*, 1750076. [CrossRef]
26. Tang, Z.; Dong, Y.; Liu, H.; Li, Z. Frequency domain analysis method of tuned liquid damper controlled multi-degree of freedoms system subject to earthquake excitation. *J. Build. Eng.* **2022**, *48*, 103910. [CrossRef]
27. Pandit, A.R.; Biswal, K.C. Seismic control of multi degree of freedom structure outfitted with sloped bottom tuned liquid damper. *Structures* **2020**, *25*, 229–240. [CrossRef]
28. Farmani, S.; Ghaeini-Hessaroeyeh, M.; Hamzehei-Javaran, S. Investigating Performance of Tuned Liquid Damper Using Finite-Element Method Based on Lagrange and Hankel Functions with Nonlinear Boundary Conditions. *J. Eng. Mech.* **2021**, *147*, 04021083. [CrossRef]